Original Research
Basic Implantodontology and Biomaterials

Bioactive glass-ceramic for bone tissue engineering: an *in vitro* and *in vivo* study focusing on osteoclasts

Rayana Longo BIGHETTI-TREVISAN[a]
Alann Thaffarell Portilho SOUZA[a]
Ingrid Wezel TOSIN[a]
Natália Pieretti BUENO[b]
Murilo Camuri CROVACE[c]
Marcio Mateus BELOTI[a]
Adalberto Luiz ROSA[a]
Emanuela Prado FERRAZ[b]

[a]Universidade de São Paulo – USP, School of Dentistry of Ribeirão Preto, Bone Research Lab, Ribeirão Preto, SP, Brazil.

[b]Universidade de São Paulo – USP, School of Dentistry, Department of Oral and Maxillofacial Surgery, Prosthesis and Traumatology, São Paulo, SP, Brazil

[c]Universidade Federal de São Carlos – UFScar, Vitreous Materials Laboratory, São Carlos, SP, Brazil.

Declaration of Interests: The authors certify that they have no commercial or associative interest that represents a conflict of interest in connection with the manuscript.

Corresponding Author:
Emanuela Prado Ferraz
E-mail: emanuelaferraz@usp.br

https://doi.org/10.1590/1807-3107bor-2022.vol36.0022

Submitted: September 10, 2020
Accepted for publication: June 2, 2021
Last revision: November 4, 2021

Abstract: Despite the crucial role of osteoclasts in the physiological process of bone repair, most bone tissue engineering strategies have focused on osteoblast-biomaterial interactions. Although Biosilicate® with two crystalline phases (BioS-2P) exhibits osteogenic properties and significant bone formation, its effects on osteoclasts are unknown. This study aimed to investigate the *in vitro* and *in vivo* effects of BioS-2P on osteoclast differentiation and activity. RAW 264.7 cells were cultured in osteoclastogenic medium (OCM) or OCM conditioned with BioS-2P (OCM-BioS-2P), and the cell morphology, viability, and osteoclast differentiation were evaluated. BioS-2P scaffolds were implanted into rat calvarial defects, and the bone tissue was evaluated using tartrate-resistant acid phosphatase (TRAP) staining and RT-polymerase chain reaction (PCR) after 2 and 4 weeks to determine the gene expressions of osteoclast markers and compare them with those of the bone grown in empty defects (Control). OCM-BioS-2P favored osteoclast viability and activity, as evidenced by an increase in the TRAP-positive cells and matrix resorption. The bone tissue grown on BioS-2P scaffolds exhibited higher expression of the osteoclast marker genes (*Ctsk*, *Mmp 9*, *Rank*) after 2 and 4 weeks and the *RankL/Opg* ratio after 2 weeks. *Trap* gene expression was lower at 2 weeks, and a higher number of TRAP-stained areas were observed in the newly formed bone on BioS-2P scaffolds at both 2 and 4 weeks compared to the Controls. These results enhanced our understanding of the role of bioactive glass-ceramics in bone repair, and highlighted their role in the modulation of osteoclastic activities and promotion of interactions between bone tissues and biomaterials.

Keywords: Biocompatible Materials; Osteoclasts; Bone and Bones; Tissue Engineering.

Introduction

The increasing clinical demand for bone regeneration has encouraged the development of porous scaffold biomaterials for tissue engineering-based therapies. The ideal biomaterial should be three-dimensional, resorbable, biocompatible, porous, and exhibit sufficient mechanical strength.[1,2] Bioactive glasses have emerged as a promising alternative due to their superior biocompatibility and osteoinductive characteristics,[3,4,5]

although their poor mechanical properties often have limited their applications.

Biosilicate®, a new bioactive glass ceramic with two crystalline phases (BioS-2P), was developed to enhance the mechanical features of glass-ceramics without affecting their biocompatibility.[6,7] BioS-2P exhibits osteoinductive and osteogenic properties which promote differentiation of the mesenchymal stem cells into osteoblasts and increase osteoblast activity *in* vitro.[8] Additionally, *in vivo* data have shown that BioS-2P is a biocompatible material with osteoconductive properties, resulting in meaningful bone formation.[8,9,10]

Studies on biomaterials in bone tissue engineering strategies have focused on osteoblast and bone formation; however, physiological bone regeneration is the result of a variety of events and is characterized by a balance between the anabolic activities of osteoblasts and catabolic activities of osteoclasts. The latter originate from hematopoietic progenitors of the macrophage cell lineage that differentiate into multinucleated cells by cell fusion. They represent a single cell type capable of degrading the mineralized matrix and play a crucial role in bone remodeling.[12,13] In the presence of biomaterials, osteoclasts migrate to scaffolds and begin the resorption process, contributing to chemical dissolution (physicochemical degradation);[14] therefore, an ideal bone substitute should affect both osteoblasts and osteoclasts to achieve effective bone remodeling.

Although variations in the physicochemical compositions of biomaterials affect the activity of osteoclasts, there is limited evidence on their interactions.[14,15,16] Although several studies have demonstrated the role of biomaterials in favoring osteogenesis in the presence of osteoclast inhibition, the actual effects of the biomaterials on osteoclasts and bone resorption are often under-explored. Thus, this study aims to evaluate the *in vitro* and *in vivo* effects of BioS-2P on osteoclast differentiation and activity to explore their role in the bone-remodeling process.

Methodology

Sample preparation and characterization

Solid discs of BioS-2P were prepared as previously described.[8] Briefly, chemical reagents composed of high-purity silica, calcium carbonate, sodium carbonate, and monosodium phosphate (JT Baker, Allentown, USA) were blended and melted at 1,350°C for 4 hours (h) to produce Biosilicate® ($24.5Na_2O$-$24.5CaO$-$45SiO_2$-$6P_2O_5$ - wt.%), followed by an additional heat treatment to obtain BioS-2P cylinder samples, which were cut into discs measuring 12 mm in diameter and 3 mm in height. The discs were ground with silicon carbide paper (grit#400), cleaned using anhydrous isopropyl alcohol in an ultrasonic cleaner for 10 minutes (min), and sterilized in dry heat at 180°C for 2 h. BioS-2P scaffolds were prepared as previously described.[17] Powered BioS-2P was mixed with carbon black (80 vol.%), dried, isostatically pressed at 200 MPa, and sintered at 975°C for 5 h. Porous scaffolds measuring 5 mm in diameter and 2 mm in height were sterilized using dry heat at 180°C for 2 h.

The disc and scaffold samples were analyzed using X-ray diffraction (XRD) (Ultima IV, Rigaku, Tokyo, Japan) from 15° to 90° in step scan mode (0.01°) with a counting time of 2 seconds (s) to confirm the presence of the crystalline phases. The powered sintered scaffolds (n = 3) and ground disc (n = 1) were analyzed, and the crystalline phases were identified using the Crystallographica Search-Match software (version 2.1.1.1) (Oxford Cryosystems, Murray Hill, USA).

Effect of osteoclastogenic medium conditioned with BioS-2P on RANKL-induced osteoclastogenesis

Preparation of osteoclastogenic medium conditioned with BioS-2P

The BioS-2P discs were first incubated with D-MEM (0.2 g/mL; Gibco, Grand Island, USA) for 24 h. The BioS-2P conditioned medium was collected and 10% fetal bovine serum (FBS, Gibco), 100 µg/mL streptomycin, 100 IU/mL penicillin (Gibco), and 50 ng/mL of RANKL (PeproTech, Rocky Hill, USA) were added to generate an osteoclastogenic medium (OCM) conditioned with BioS-2P (OCM-BioS-2P). OCM unexposed to BioS-2P was used as control (OCM-Control). The OCM-BioS-2P was freshly produced every 48 h to change the medium of the cell cultures.

Cell culture

The RAW 264.7 mouse macrophage cell line (ATCC, Manassas, USA) was cultured with OCM-BioS-2P or OCM-Control. The cells were seeded at the following densities, according to the experiment: cell morphology analysis: $1x10^4$ on Thermanox® coverslips (Nunc, Rochester, USA) in 24-well plates (Corning Inc, Corning, USA); osteoclast viability and activity assays: $5x10^3$ in 96-well plates (Corning); resorption assay: $5x10^3$ in Osteo Assay 96-well Strip Plate (Corning). The cells were kept in a 5% CO_2 incubator at 37°C, the medium was changed every 48 h and the culture progression was evaluated using an inverted phase microscope (Zeiss, Jena, Germany).

Cell morphology

Cell morphology was assessed by direct fluorescence. After 24 and 72 h, the cells exposed to OCM-BioS-2P and OCM-Control were fixed in 4% paraformaldehyde (Merck, Darmstadt, Germany) for 10 min and permeabilized with Triton X-100 0.5% (Acros Organics, Geel, Belgium). Alexa Fluor 488 conjugated with phalloidin (Molecular Probes, Eugene, USA) 1:200, and 4',6-diamidino-2-phenylindole, dihydrochloride 300 (DAPI) (Molecular Probes) were used to stain the actin cytoskeleton and nuclei, respectively. Cell morphology was examined under epifluorescence using an Axio Imager microscope (Zeiss) attached to an AxionCam MRm (Zeiss) digital camera. The images were merged using the AxionVision 4.8 software (Zeiss) (n = 3).

Cell viability

Cell viability was assessed using a 3-[4,5-dimethylthiazol-2-yl]-2,5-diphenyl tetrazolium bromide] (MTT) (Sigma-Aldrich, St Louis, USA) assay. After 3, 5, and 7 days, cells were incubated with 5 mg/mL of MTT in phosphate buffered saline (PBS, Gibco) at 37°C for 4 h. The solution was replaced by acidified isopropanol [0.04 N HCl in isopropanol (Merck)] and agitated for 5 min. The absorbance was measured as optical density at 570 nm (n = 5) using a μQuant plate reader (Biotek, Winooski, USA). Wells without cells were used as baseline zero.

Osteoclast activity

a. *TRAP staining assay*: After 5 days, tartrate-resistant acid phosphatase (TRAP) stain analysis was performed using the leukocyte acid phosphatase kit (procedure 387, Sigma-Aldrich) according to the manufacturer's protocol. Briefly, the medium was removed, cells were washed at 37°C with deionized water, and fixed for 30 s, at room temperature (RT). Thereafter, the cells were stained with TRAP staining solution and incubated at 37°C in humidified atmosphere. After 1 h, the cells were washed with 37°C deionized water and dried at RT. The images of five wells in each group were acquired using a stereomicroscope coupled to a Leica DC 300F high-resolution digital camera (Leica Biosystem, Wetzlar, Germany), and the TRAP-stained areas were quantified by pixel count using a LASV 4.0 Image Analysis Software (Leica). Data were expressed as a percentage of the total area (n = 5).
b. *Resorption assay*: The cells were cultured in an Osteo Assay Stripwell Plate (Corning) using expansion medium for 24 h to allow cell adhesion. Subsequently, the medium was changed to OCM-BioS-2P or OCM-Control (n = 5). As negative controls, wells were incubated with OCM-BioS-2P (n = 2) or OCM-Control (n = 2) in the absence of cells. After 7 days, 2.5% sodium hypochlorite bleaching solution (Rioquímica, São José do Rio Preto, Brazil) was added to remove adhered cells, and the wells were washed and dried at RT. The images were acquired using a stereomicroscope coupled to a Leica DC 300F high-resolution digital camera (Leica), and resorption areas were quantified using the LASV 4.0 Image Analysis Software (Leica). Data were expressed as a percentage of the total area (n=5).

Effect of BioS-2P on *in vivo* osteoclast activity

All procedures were conducted under the guidelines of the Committee of Ethics in Animal Research of the University of São Paulo (#2016.1.840.58.8). The sample size was calculated based on our previously published studies that

used the same experimental model and analyses,[8,18] assuming 95% confidence interval or 5% level of significance and according to the ethical and "3R's" principles of animal experimentation.

Surgical implantation of BioS-2P scaffold

Forty male Wistar rats weighing 150–200 g were anesthetized using an intraperitoneal injection containing 7 mg/100 g of Ketamine (Agener União, São Paulo, Brazil) and 0.6 mg/100 g of Xylazine (Calier, Osasco, Brazil). A surgical incision was made to expose the parietal bone. A trephine bur was used to create an unilateral 5-mm diameter bone defects that were immediately implanted with BioS-2P scaffolds, followed by a skin suture. The animals were treated with single doses of intramuscular antibiotics (50.000 UI/kg, Pentabiotic; Fort Dodge, Campinas, Brazil) and anti-inflammatory analgesics [Flunixin meglumine (0.25 mg/100 g); Schering-Plough, Union, USA]. Empty defects were used as controls. The animals were euthanized after 2 and 4 weeks and the calvariae were harvested for evaluation of gene expression (n = 5 animals per period and group, total n = 20 animals) and histological and histochemical analysis (n = 5 animals per period and group, total n = 20 animals).

Gene expression of osteoclast markers

Quantitative real-time polymerase chain reaction (PCR) was carried out at 2 and 4 weeks to evaluate the gene expression of tartrate-resistant acid phosphatase (*Trap*), cathepsin K (C*tsk*), matrix metallopeptidase 9 (M*mp9*), receptor activator of nuclear factor kappa B (R*ank*), rank ligand (R*ankL*), and osteoprotegerin (O*pg*). The total RNA was extracted using Trizol (Invitrogen, Carlsbad, USA) and isolated using an SV Total RNA Isolation Kit (Promega, Madison, USA) according to the manufacturer's instructions. RNA concentration and purity were evaluated using a GeneQuant® spectrophotometer (GE Healthcare, Chicago, USA), and integrity was examined using the 2100 Bioanalyzer (Agilent Technologies, Santa Clara, USA). A complementary DNA (cDNA) was synthesized with a High Capacity Kit (Invitrogen) using 1 mg of total RNA through a reverse transcription reaction. Real-time PCR was conducted in a Step One Plus Real-Time PCR System (Thermo Fisher, Waltham, USA) using the Taqman PCR Master Mix (Thermo Fisher) and selected probes for the target genes (Thermo Fisher) (n = 4; Table 1). To generate precise and reliable data, four candidate housekeeping genes (*Actb*, *Gapdh*, *Rplp-2*, *Hprt1*) were evaluated using RT-PCR, and the *Rplp-2* was selected based on its expression stability in all groups. The gene expression was normalized by *Rplp-2*, and the changes were relative to gene expression of the control group at 2 weeks using the $2^{-\Delta\Delta Ct}$ method.[19]

TRAP staining

TRAP staining was performed at 2 and 4 weeks to evaluate the osteoclastic activity of newly formed bone in contact with the BioS-2P scaffolds and to compare it with that of the control defects. The harvested calvariae were fixed in formalin (Merck), decalcified in buffered Ethylenediaminetetraacetic acid (Merck), dehydrated in an ethanol series (Merck), and embedded in paraffin (Merck). Five-micrometer thick sections were obtained from the central regions of the samples and five histological sections from each animal were selected, resulting in 25 sections for each group and experimental time. All histological sections were stained using the TRAP kit (Sigma-Aldrich) and counterstained

Table 1. Predesigned TaqMan Probes.

Target gene	Acession n°	Amplicon lenght
Trap	Rn00569608_m1	95
Ctsk	Rn00580723_m1	69
Mmp9	Rn00579162_m1	72
Rank	Rn04340164_m1	63
RankL	Rn00589289_m1	69
Opg	Rn00563499_m1	75
Rplp2	Rn01479927_m1	130

Trap: tartrate-resistant acid phosphatase, Ctsk: cathepsin K, Mmp9: matrix metallopeptidase 9, Rank: receptor activator of nuclear factor kappa B, RankL: Rank ligand, Opg: osteoprotegerin and Rplp2: ribosomal protein lateral stalk subunit P2.

with 1% light green (Merck) according to the manufacturer's protocol. To ensure that all stained areas across the section is counted, images were obtained at 10x magnification from the two edges and the center of the defects. These images were acquired using a light microscope (Leica) coupled to a digital camera (Leica). Positive TRAP areas were quantified by pixel counting and expressed as a percentage of the total tissue area using the LASV 4.0 Image Analysis Software (Leica). For qualitative evaluation, images at 40x magnification were also acquired following the same protocol.

Hematoxylin and Eosin (H&E) and Masson's Trichrome (MT) staining

For qualitative evaluation of the microstructure of the bone and connective tissues surrounding the BioS-2P after 4 weeks, the samples were processed as described above and the histological sections were stained with H&E (Merck) and Masson's Trichrome (Merck) according to the manufacturer's protocol. Images were obtained using a light microscope (Leica) attached to a digital camera (Leica).

Bone formation and BioS-2P resorption

The amount of new bone and the rate of BioS-2P degradation were evaluated using histometric analysis. For this, 10x magnification images of three sections per group/per animal were selected (H&E), and the measurements were performed using the GRID plugin of the Image-J software (National Institutes of Health, Bethesda, USA) containing 108 equidistant intersection points (with a per point area of 2,600 μm^2). The grid was positioned over the image, and the points that overlapped the newly formed bone and BioS-2P were counted. Data were expressed as percentages of the total number of points.

Statistical analysis

The quantitative data were compared using parametric t-test or analysis of variance (ANOVA) followed by the Student-Newman-Keuls test when indicated (Sigma Plot 11.0 Systat Software Inc., San Jose, USA). The significance level was set at 5% ($p \leq 0.05$).

Results

BioS-2P presents two crystalline phases composed of sodium calcium silicate ($Na_2CaSi_2O_6$) and sodium calcium phosphate ($NaCaPO_4$; a secondary crystalline phase) crystals (approximately 5 vol. %) that grow at the grain boundaries of the main phase ($Na_2CaSi_2O_6$). These crystalline phases were identified on both scaffolds and solid discs, and no signs of residual amorphous phase were detected. The XRD spectra confirmed that the main crystalline phase in BioS-2P was $Na_2CaSi_2O_6$, followed by $NaCaPO_4$ that presented three main diffraction peaks at 23.3°C, 32.7°C, and 47.5°C (Figure 1). The lower peak intensity of the second crystalline phase indicated lower crystallized volume fraction (Figure 1).

Effect of OCM-BioS-2P on RANKL-induced osteoclastogenesis

No noticeable differences in cell morphology were observed after 24 and 72 h of incubation in OCM-Control and OCM-BioS-2P cultures (Figure 2). At 24 h, RAW 264.7 cells were predominantly round-shaped, surrounded by a ring of actin filaments with few extensions at the cell edges (Figures 2A and C). After 72 h, the cells exhibited a morphological modification

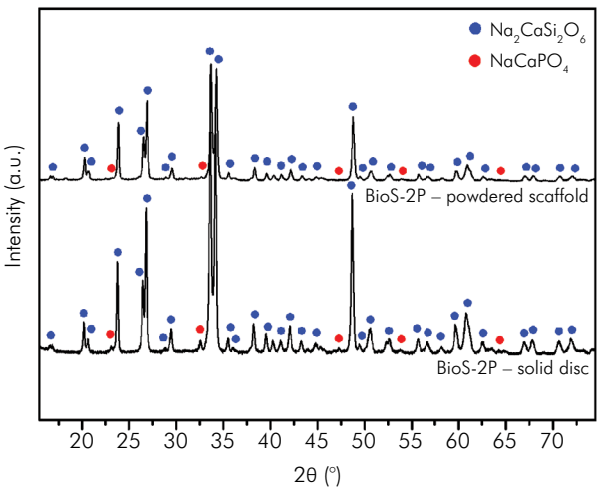

Figure 1. X-ray diffraction (XRD) patterns of solid discs of Biosilicate® with two crystalline phases (BioS-2P) and BioS-2P powdered scaffolds, showing the presence of both sodium calcium silicate ($Na_2CaSi_2O_6$) and sodium calcium phosphate ($NaCaPO_4$) crystalline phases.

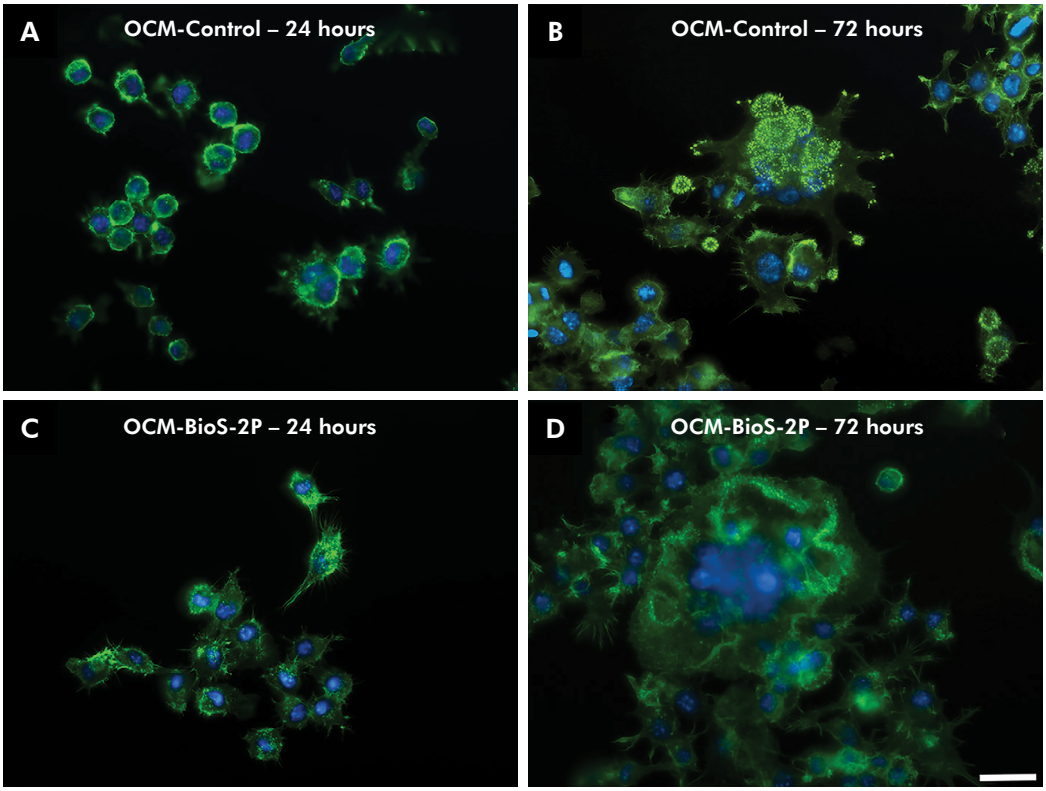

Figure 2. Effect of osteoclastogenic medium (OCM) conditioned with Biosilicate® with two crystalline phases (OCM-BioS-2P) on RAW 264.7 cell morphology, compared to OCM-Control (OCM-Control). RAW 264.7 incubated with OCM-Control (OCM-Control) for (A) 24 hours and (B) 72 hours. RAW 264.7 incubated with OCM-BioS-2P for (C) 24 hours and (D) 72 hours. Magnification: 40X. Scale bar: 50 mm.

evidenced by multiple cytoplasmic projections and cell fusion, indicating that osteoclast differentiation was induced by RANKL irrespective of the presence of OCM-BioS-2P (Figures 2B and D).

Cell viability significantly differed between experimental periods after treatment (Figure 3A; two-way ANOVA, $p = 0.013$). While no differences were noticed between the groups on day 3, the cultures of OCM-BioS-2P favored viability on days 5 and 7. Conversely, no significant changes in cell viability were detected in OCM-Control cultures from days 3 to 5, although a decline was evident on day 7. Furthermore, cells incubated with OCM-BioS-2P presented a peak viability on day 5 that remained unaltered until day 7 (Figure 3A).

Cultures incubated with OCM-BioS-2P presented significantly higher TRAP staining areas compared to those incubated with OCM-Controls (t-test, $p = 0.004$, Figure 3B). Furthermore, the resorption pits and quantified resorbed areas were significantly more evident in cultures grown on OCM-BioS-2P compared to those in OCM-Controls (t-test, $p = 0.007$, Figure 3C). Overall, these data indicated that OCM-BioS-2P favored osteoclast differentiation and activity.

Effect of BioS-2P on *in vivo* osteoclast activity

None of the animals presented any surgical complications, and the postoperative period was uneventful. The RNA isolation and extraction method ensured RNA samples with RNA integrity number (RIN) over 7.1, which was suitable for gene expression analysis (Table 2). All evaluated genes exhibited decreased expression in both groups from 2 to 4 weeks (Figure 4). The gene expression of *Trap* was significantly higher in the control group than in the experimental group at 2 weeks, while no difference was noticed between the groups at

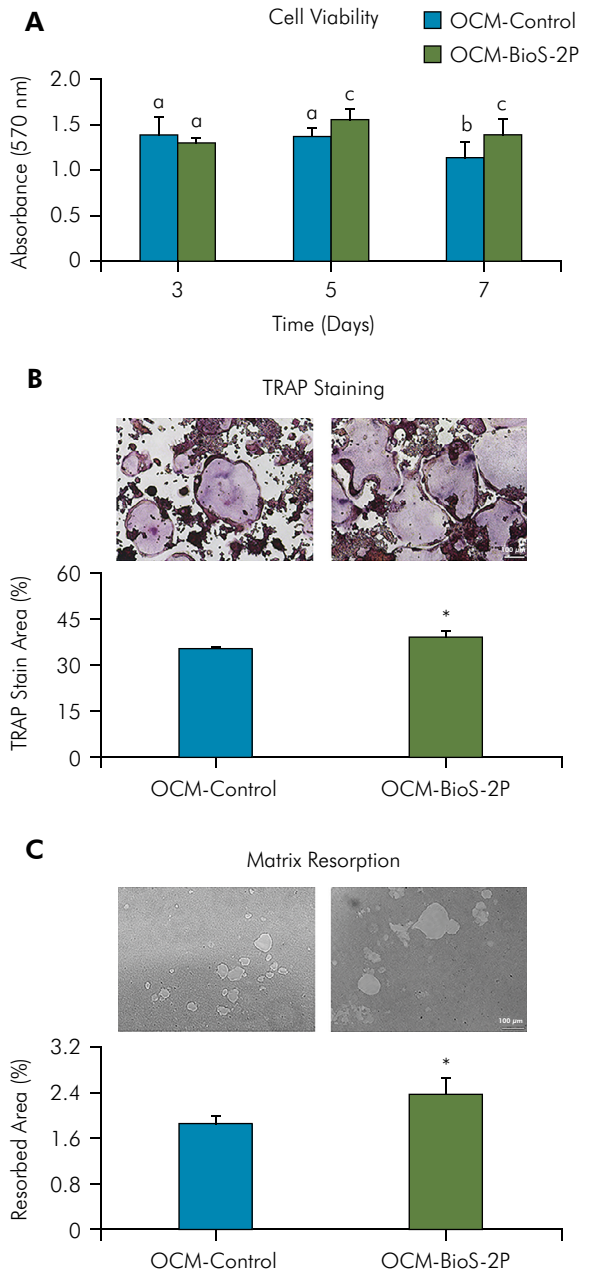

Figure 3. Effect of osteoclastogenic medium (OCM) conditioned with Biosilicate® with two crystalline phases (OCM-BioS-2P) on cell viability and osteoclast activity, compared to OCM-Control (OCM-Control). (A) Cell viability was higher in cultures incubated with OCM-BioS-2P for 5 and 7 days. (B) Representative images and percentage of areas stained by tartrate-resistant acid phosphatase (TRAP) in cells incubated with OCM-BioS-2P compared to OCM-Control at 5 days. (C) Representative images of resorption pits and percentage of resorbed areas of cells incubated with OCM-BioS-2P compared to OCM-Control at 7 days. Data are presented as mean ± standard deviation (n = 5). Different letters and asterisks (*) indicate statistically significant differences ($p \leq 0.05$). Magnification: 10X. Scale bar: 200 mm.

Table 2. RNA integrity number of newly formed bone in calvariae defects implanted with BioS-2P and without treatment (Control) after 2 and 4 weeks.

	Control		BioS-2P	
Time (weeks)	2	4	2	4
RIN	7.1	8.4	7.4	7.6
n	5	5	5	5

4 weeks (Figure 4, one-way ANOVA: $p < 0.001$). Significantly higher expressions of *Ctsk*, *Mmp9*, and *Rank* (Figure 4, one-way ANOVA: $p < 0.001$ for all genes) were detected in the experimental group compared to the control group at both 2 and 4 weeks. The *RankL* / *Opg* ratio was significantly higher in the experimental group than in the control group at 2 weeks, while no difference was noticed at 4 weeks (Figure 4, one-way ANOVA: $p < 0.001$).

Histological analyses of the edges of the bone defects in the control group revealed lamellar bone tissue adjacent to TRAP-stained areas at 2 and 4 weeks (Figures 5A and B). Conversely, the experimental group exhibited a higher amount of TRAP-stained areas at the edges of the defects, particularly after 4 weeks (Figures 5C and D). Quantification of the TRAP areas confirmed the histological evidence, with the TRAP areas at the edges of the control defects being similar from 2 to 4 weeks in the control group and increasing over time (4 > 2 weeks) in the experimental group. Although, no differences were observed between the groups at 2 weeks, the TRAP areas were higher in the BioS-2P group compared to the control group (Figure 5E, one-way ANOVA: $p = 0.039$) at 4 weeks.

A fibrous tissue of varying density was noticed at the center of the defects and the presence of TRAP-stained areas was few and scattered, especially at 2 weeks (Figures 6A and B). TRAP-stained areas were present at the center of the defect and in contact with the BioS-2P at both 2 and 4 weeks in the experimental group (Figures 6C and D), and quantification of these areas confirmed the histological evidence. The TRAP area was higher at the center of the defect in the experimental group compared to the control group at both 2 and 4 weeks (Figure 6E, one-way ANOVA: $p = 0.023$).

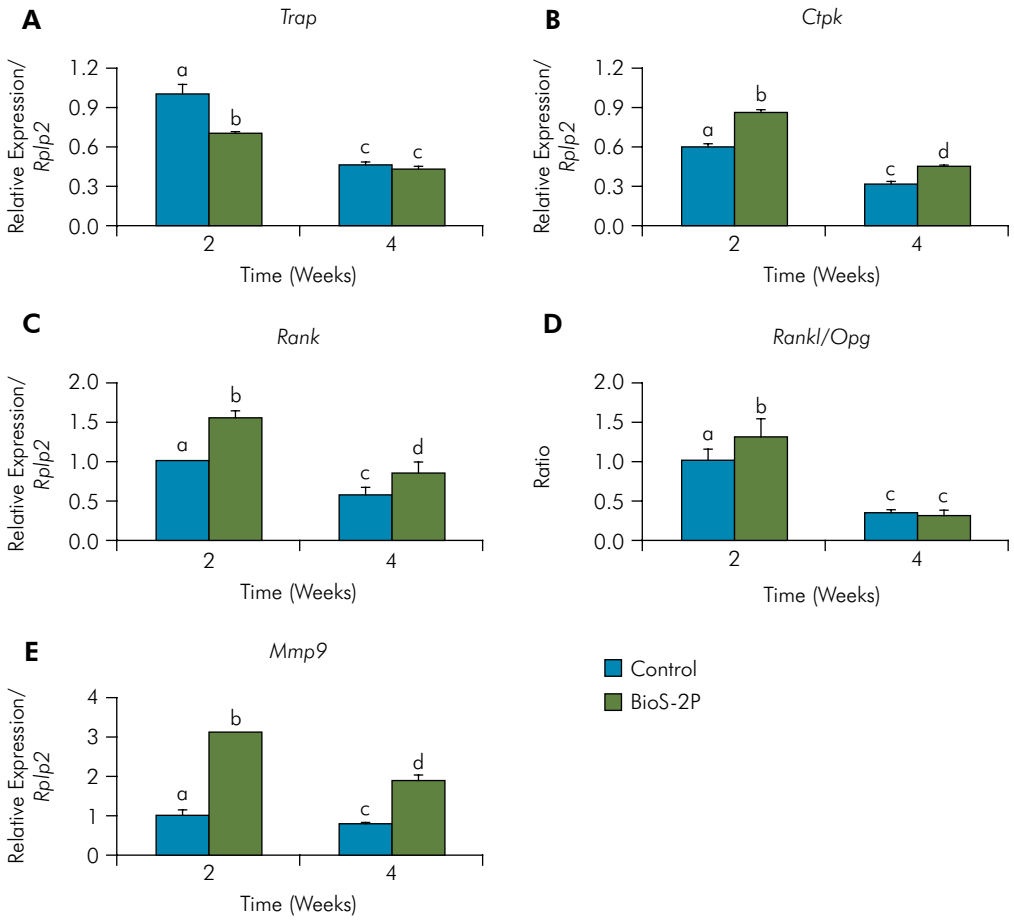

Figure 4. Relative gene expression of the osteoclast markers, tartrate-resistant acid phosphatase (*Trap*), cathepsin K (*Ctpk*), metalloprotease 9 (*Mmp9*), receptor activator of nuclear factor kappa-B (*Rank*), RANK ligand (*Rankl*), and osteoprotegerin (*Opg*) of the newly formed bone in rat calvarial defects without treatment (Control) or implanted with Biosilicate® with two crystalline phases (BioS-2P) after 2 and 4 weeks. Data are presented as mean ± standard deviation (n = 4). Bars with different letters are significantly different ($p \leq 0.05$).

To confirm bone formation and biomaterial resorption as well as the presence of osteoclasts surrounding the BioS-2P surface, histological analyses including H&E and MT staining were performed. The osteoclastic activity was followed by bone formation. The amount of new bone increased in both groups from 2 to 4 weeks, being higher in the BioS-2P group compared to the control group (Figure 7A, two-way ANOVA: $p < 0.001$ for period and $p = 0.01$ for groups); moreover, the bone formation in the BioS-2P group was accompanied by a decrease in the amount of biomaterial (Figure 7B, t-test: $p = 0.006$). A highly cellular osteoid matrix with numerous blood vessels in both groups indicated active bone formation (Figures 8A–E, G–K). In the experimental group, the presence of non-resorbed biomaterial (Figures 8E and K) surrounded by osteoclasts (Figures 8F and L) was evident.

Discussion

Recent studies have demonstrated that BioS-2P is a suitable biomaterial to be used as a bone substitute that creates promising micro-environmental conditions to promote bone formation.[8] This study investigated the effects of BioS-2P on bone resorption using *in vitro* and *in vivo* models, and the findings revealed that it favored osteoclast differentiation and activity while supporting bone formation.

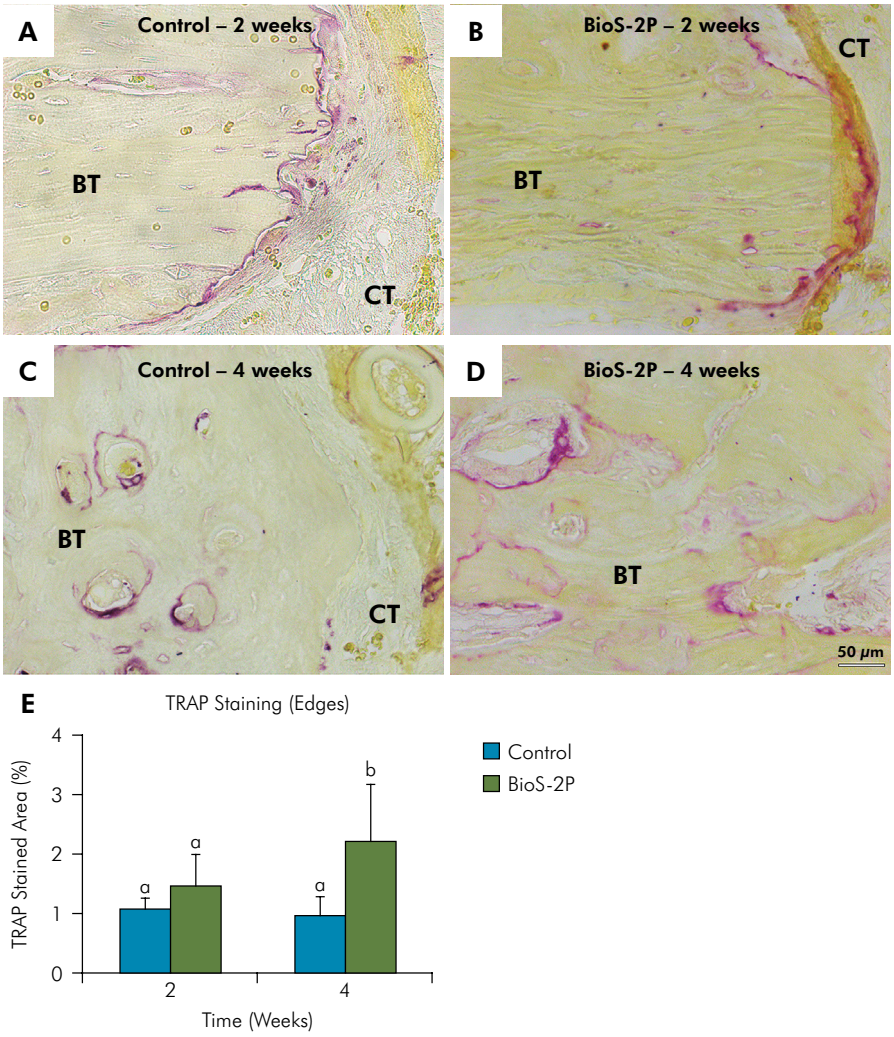

Figure 5. Representative images of histological sections of samples stained with tartrate-resistant acid phosphatase (TRAP) from the edges of the rat calvarial defects without treatment (Control, A-B) or implanted with Biosilicate® with two crystalline phases (BioS-2P, C-D) after 2 and 4 weeks. Magnification: 40X. Scale bar: 50 mm. Quantitative data expressed as relative TRAP-stained area at the edges of the rat calvarial bone defects without treatment (Control) or implanted with BioS-2P after 2 and 4 weeks (E). Data are presented as mean ± standard deviation (n = 5). Bars with different letters are significantly different ($p \leq 0.05$).

RAW 264.7 is a mouse macrophage cell line commonly used in osteoclastic signaling pathways and biomaterial studies, and different culture conditions may affect cell viability, differentiation, and activity.[20] After culturing for 72 h with OCM-BioS-2P and OCM-Control, multinucleated cells and an actin ring were observed without differences in cell morphology, irrespective of the culture medium used. This was similar to the results observed when RAW 264.7 cells were exposed to a mesoporous bioactive glass.[21]

Although the cell morphology was similar, higher cell viability combined with the amount of TRAP staining indicated that OCM-BioS-2P favored culture growth and resulted in increased resorptive activity: the final event of osteoclast differentiation. The existing literature on the relationship between bioactive glasses and osteoclast activity is contradictory.[20,21,22,23,24] While some studies found bone erosion to be superficial, indicated by the formation of poorly outlined rims created by the cells,[20,21,22] others reported evidence of increased osteoclast differentiation and activity.[23,24] This contradiction may be due to differences in the experimental models, fabrication routes, and chemical compositions of the biomaterials used.

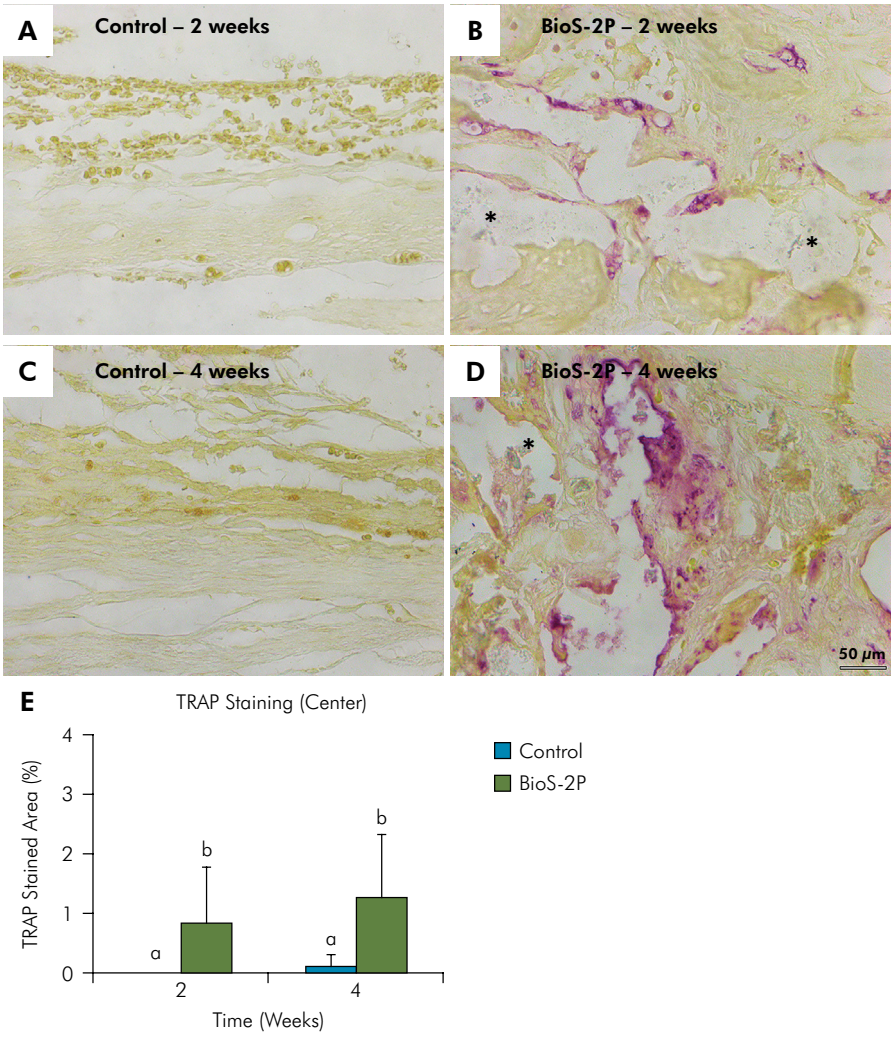

Figure 6. Representative images of histological sections of samples stained with tartrate-resistant acid phosphatase (TRAP) at the center of the rat calvarial bone defects without treatment (Control, A-B) or implanted with Biosilicate® with two crystalline phases (BioS-2P, C-D) after 2 and 4 weeks. Magnification: 40X. Scale bar: 50 mm. Quantitative data expressed as relative TRAP-stained area at the center of the rat calvarial bone defects without treatment (Control) or implanted with BioS-2P after 2 and 4 weeks (E). Data are presented as mean ± standard deviation (n = 5). Bars with different letters are significantly different ($p \leq 0.05$).

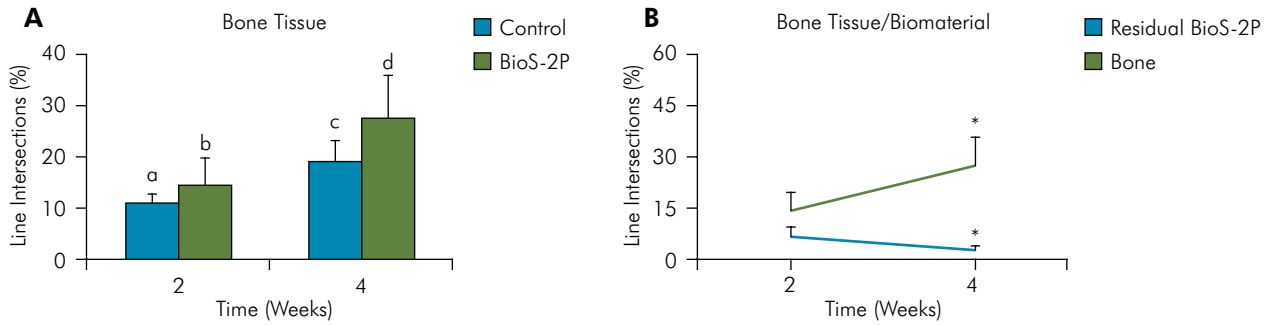

Figure 7. Percentages of points (line intersection) in newly formed bone on rat calvarial bone defects without treatment (Control) or implanted with Biosilicate® with two crystalline phases (BioS-2P) after 2 and 4 weeks (A). Percentages of points (line intersection) in the newly formed bone or residual biomaterial on BioS-2P group after 2 and 4 weeks (B). Data are presented as mean ± standard deviation (n=5). Bars with different letters are significantly different ($p \leq 0.05$). (*) Asterisk indicates differences between periods in the same group.

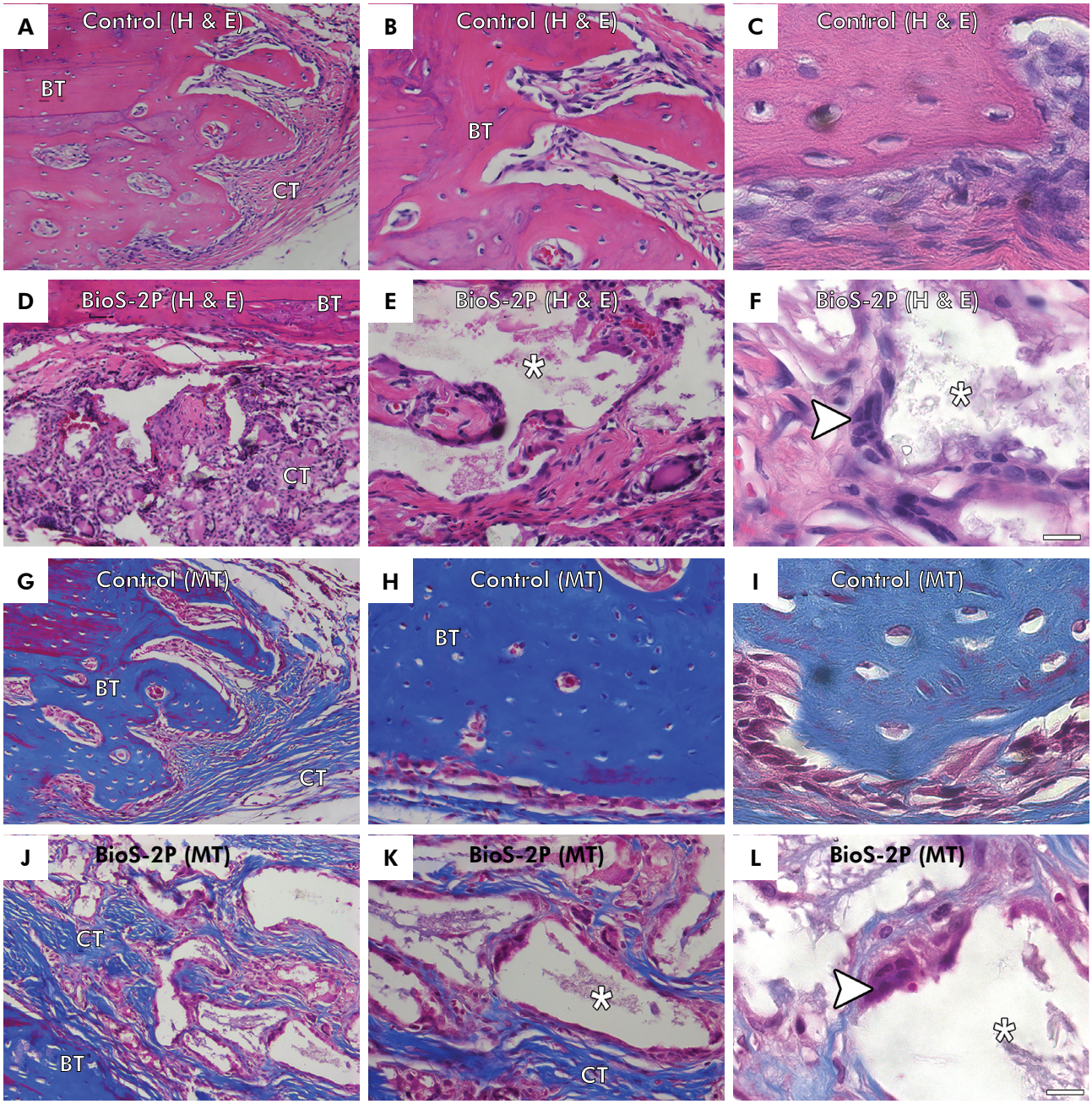

Figure 8. Representative images of histological sections of samples stained with hematoxylin-eosin (H&E) (A–F) and Masson's trichrome (MT) (G–L) in rat calvarial bone defects without treatment (Control, A–C, G–I) or implanted with Biosilicate® with two-crystalline phases scaffolds (BioS-2P, D–F, J–L) after 4 weeks. BT: bone tissue; CT: connective tissue; (*) asterisk: non-resorbed scaffold; arrows: osteoclasts. Magnifications and scale bars: A, D, G, and J (20X, 100 mm); B, E, H, and K (40X, 50 mm); C, F, I, and L (100X, 20 mm).

Bioactive glass and glass ceramic-based materials, including BioS-2P, stimulate the gene expression of osteogenic markers, angiogenic factors, and antibacterial activity, which can be due to the presence of ionic dissolution products.[15,25,26,27,28,29] Metal ions have been added to the composition of biomaterials to improve bone formation as inorganic ions decrease osteoclast activity.[22,30,31,32] Biosilicate® is mainly composed of calcium, phosphorous, sodium, and silicon oxides, and the lack of metal ions could

explain its stimulatory effect on osteoclast activity.[7] Our findings are in agreement with the previously published results, where bioactive glasses with a similar ionic composition increased the osteoclastic differentiation of RAW 264.7 cells.[20]

The physicochemical properties of the scaffolds used as bone substitutes may also affect *in vivo* osteoclastogenesis.[14,33] A previous study reported a significant amount of osteoclasts in contact with the bioglass material surface, corroborating our findings.[34] Additionally, the presence of increased TRAP-stained areas in the bone contacting BioS-2P may indicate a similar effect of dissolution products on osteoclast precursors.

We also evaluated the cellular differentiation and gene expression of key markers of osteoclasts in the new bone. The isolation of high-quality RNA from *in vivo* samples can be challenging due to material degradation and may result in unreliable gene expression data. Also, the isolation method may contribute to RNA degradation; however, RIN values higher than 7.0 are usually considered acceptable.[35,36] The *Ctsk*, *Trap*, *Rank,* and *Mmp9* genes are related to osteoclastogenesis, while the *RankL/Opg* ratio refers to the kinetics of remodeling. The findings revealed overexpression of most of these genes, indicating that the bone tissue grown in contact with BioS-2P exhibited remodeling activity.

The correlation between the expression levels of protein and mRNA has been discussed elsewhere,[37] and the absence of a positive relation between the *Trap* gene and TRAP protein expressions could be due to the experimental model, period of evaluation, post-transcriptional events, and the presence of biomaterials that could alter some genetic pathways.[28,38] Even though *Trap* gene expression was decreased, TRAP staining, a specific histochemical marker that directly reflects the osteoclastic activity and function,[14,39,40] was enhanced in the BioS-2P group, suggesting that a higher number of osteoclasts were in contact with the biomaterial.

Bone regeneration involves synergistic and controlled actions between the formation and resorption processes. A key focus of tissue engineering strategies is the development of a bone substitute that is completely biodegradable within an adequate period and with a balance between the biomaterial resorption and bone formation rates. The results of this study confirmed the osteoconductive properties of BioS-2P, evidenced by the presence of an increased amount of bone at both the center and edges of the defect in the experimental group from 2 to 4 weeks when compared to the Control group.[8] Also, a decrease in the amount of biomaterial was observed over time, although not at the same rate compared to bone formation, which could explain the presence of traces of the material 12 weeks post-implantation in rat calvarial defects.[8]

Conclusion

The development of functional scaffolds to control bone remodeling is essential for achieving bone regeneration. In addition to its role in bone formation, the findings of this study revealed that BioS-2P affected osteoclast differentiation and activity, thus confirming its suitability as a biomaterial for bone tissue engineering strategies. Further studies can contribute to the investigation on the molecular mechanisms involved in the osteoblast-osteoclast-BioS-2P circuit that could eventually affect bone response in the presence of Biosilicate®.

Acknowledgments

This research was supported by grants from CNPq (406526/2018-4) and FAPESP (2016/22528-5). We would like to thank Roger Rodrigo Fernandes and Adriana Luísa Gonçalves de Almeida for their assistance during the experiments.

References

1. Bose S, Roy M, Bandyopadhyay A. Recent advances in bone tissue engineering scaffolds. Trends Biotechnol. 2012 Oct;30(10):546-54. https://doi.org/10.1016/j.tibtech.2012.07.005

2. Tang D, Tare RS, Yang LY, Williams DF, Ou KL, Oreffo RO. Biofabrication of bone tissue: approaches, challenges and translation for bone regeneration. Biomaterials. 2016 Mar;83:363–82. https://doi.org/10.1016/j.biomaterials.2016.01.024
3. Hench LL. Bioceramics. J Am Ceram Soc. 1998 May;81(7):1705–28. https://doi.org/10.1111/j.1151-2916.1998.tb02540.x
4. Hench LL, Xynos ID, Polak JM. Bioactive glasses for in situ tissue regeneration. J Biomater Sci Polym Ed. 2004;15(4):543–62. https://doi.org/10.1163/156856204323005352
5. Hench LL, Jones JR. Bioactive Glasses: frontiers and Challenges. Front Bioeng Biotechnol. 2015 Nov;3:194. https://doi.org/10.3389/fbioe.2015.00194
6. Peitl O, Zanotto ED, Hench LL. Highly bioactive P2O5–Na2O–CaO–SiO2 glass-ceramics. J Non-Cryst Solids. 2001 Nov;292(1-3):115–26. https://doi.org/10.1016/S0022-3093(01)00822-5
7. Peitl O, Zanotto ED, Serbena FC, Hench LL. Compositional and microstructural design of highly bioactive P2O5-Na2O-CaO-SiO2 glass-ceramics. Acta Biomater. 2012 Jan;8(1):321–32. https://doi.org/10.1016/j.actbio.2011.10.014
8. Prado Ferraz E, Pereira Freitas G, Camuri Crovace M, Peitl O, Dutra Zanotto E, de Oliveira PT, et al. Bioactive-glass ceramic with two crystalline phases (BioS-2P) for bone tissue engineering. Biomed Mater. 2017 Aug;12(4):045018. https://doi.org/10.1088/1748-605X/aa768e
9. Roriz VM, Rosa AL, Peitl O, Zanotto ED, Panzeri H, de Oliveira PT. Efficacy of a bioactive glass-ceramic (Biosilicate) in the maintenance of alveolar ridges and in osseointegration of titanium implants. Clin Oral Implants Res. 2010 Feb;21(2):148–55. https://doi.org/10.1111/j.1600-0501.2009.01812.x
10. Kido HW, Tim CR, Bossini PS, Parizotto NA, de Castro CA, Crovace MC, et al. Porous bioactive scaffolds: characterization and biological performance in a model of tibial bone defect in rats. J Mater Sci Mater Med. 2015 Feb;26(2):74. https://doi.org/10.1007/s10856-015-5411-9
11. Eriksen EF. Normal and pathological remodeling of human trabecular bone: three dimensional reconstruction of the remodeling sequence in normals and in metabolic bone disease. Endocr Rev. 1986 Nov;7(4):379–408. https://doi.org/10.1210/edrv-7-4-379
12. Teitelbaum SL. Bone resorption by osteoclasts. Science. 2000 Sep;289(5484):1504–8. https://doi.org/10.1126/science.289.5484.1504
13. Feng X, Teitelbaum SL. Osteoclasts: new Insights. Bone Res. 2013 Mar;1(1):11–26. https://doi.org/10.4248/BR201301003
14. Detsch R, Boccaccini AR. The role of osteoclasts in bone tissue engineering. J Tissue Eng Regen Med. 2015 Oct;9(10):1133–49. https://doi.org/10.1002/term.1851
15. Baino F, Hamzehlou S, Kargozar S. Bioactive Glasses: Where Are We and Where Are We Going? J Funct Biomater. 2018 Mar;9(1):25. https://doi.org/10.3390/jfb9010025
16. Steffi C, Shi Z, Kong CH, Wang W. Modulation of Osteoclast Interactions with Orthopaedic Biomaterials. J Funct Biomater. 2018 Feb;9(1):18. https://doi.org/10.3390/jfb9010018
17. Kido HW, Oliveira P, Parizotto NA, Crovace MC, Zanotto ED, Peitl-Filho O, et al. Histopathological, cytotoxicity and genotoxicity evaluation of Biosilicate® glass-ceramic scaffolds. J Biomed Mater Res A. 2013 Mar;101(3):667–73. https://doi.org/10.1002/jbm.a.34360
18. Lopes HB, Ferraz EP, Almeida AL, Florio P, Gimenes R, Rosa AL, et al. Participation of MicroRNA-34a and RANKL on bone repair induced by poly(vinylidene-trifluoroethylene)/barium titanate membrane. J Biomater Sci Polym Ed. 2016 Sep;27(13):1369–79. https://doi.org/10.1080/09205063.2016.1203217
19. Livak KJ, Schmittgen TD. Analysis of relative gene expression data using real-time quantitative PCR and the 2(-Delta Delta C(T)) Method. Methods. 2001 Dec;25(4):402–8. https://doi.org/10.1006/meth.2001.1262
20. Detsch R, Rübner M, Strissel PL, Mohn D, Strasser E, Stark WJ, et al. Nanoscale bioactive glass activates osteoclastic differentiation of RAW 264.7 cells. Nanomedicine (Lond). 2016 May;11(9):1093–105. https://doi.org/10.2217/nnm.16.20 PMID:27092984
21. Gómez-Cerezo N, Casarrubios L, Morales I, Feito MJ, Vallet-Regí M, Arcos D, et al. Effects of a mesoporous bioactive glass on osteoblasts, osteoclasts and macrophages. J Colloid Interface Sci. 2018 Oct;528:309–20. https://doi.org/10.1016/j.jcis.2018.05.099
22. Gómez-Cerezo N, Verron E, Montouillout V, Fayon F, Lagadec P, Bouler JM, et al. The response of pre-osteoblasts and osteoclasts to gallium containing mesoporous bioactive glasses. Acta Biomater. 2018 Aug;76:333–43. https://doi.org/10.1016/j.actbio.2018.06.036
23. Midha S, Bergh W, Kim TB, Lee PD, Jones JR, Mitchell CA. Bioactive glass foam scaffolds are remodelled by osteoclasts and support the formation of mineralized matrix and vascular networks in vitro. Adv Healthc Mater. 2013 Mar;2(3):490–9. https://doi.org/10.1002/adhm.201200140
24. Höner M, Lauria I, Dabhi C, Kant S, Leube RE, Fischer H. Periodic microstructures on bioactive glass surfaces enhance osteogenic differentiation of human mesenchymal stromal cells and promote osteoclastogenesis in vitro. J Biomed Mater Res A. 2018 Jul;106(7):1965–78. https://doi.org/10.1002/jbm.a.36399
25. Xynos ID, Edgar AJ, Buttery LD, Hench LL, Polak JM. Gene-expression profiling of human osteoblasts following treatment with the ionic products of Bioglass 45S5 dissolution. J Biomed Mater Res. 2001 May;55(2):151–7. https://doi.org/10.1002/1097-4636(200105)55:2<151::AID-JBM1001>3.0.CO;2-D

26. Gorustovich AA, Roether JA, Boccaccini AR. Effect of bioactive glasses on angiogenesis: a review of in vitro and in vivo evidences. Tissue Eng Part B Rev. 2010 Apr;16(2):199–207. https://doi.org/10.1089/ten.teb.2009.0416
27. Hu S, Chang J, Liu M, Ning C. Study on antibacterial effect of 45S5 Bioglass. J Mater Sci Mater Med. 2009 Jan;20(1):281–6. https://doi.org/10.1007/s10856-008-3564-5
28. Martins CS, Ferraz EP, De Castro-Raucci LM, Teixeira LN, Maximiano WM, Rosa AL, et al. Changes in actin and tubulin expression in osteogenic cells cultured on bioactive glass-based surfaces. Microsc Res Tech. 2015 Nov;78(11):1046–53. https://doi.org/10.1002/jemt.22583
29. Ferraz EP, Oliveira FS, Oliveira PT, Crovace MC, Peitl-Filho O, Beloti MM, et al. Bioactive glass-based surfaces induce differential gene expression profiling of osteoblasts. J Biomed Mater Res A. 2017 Feb;105(2):419–23. https://doi.org/10.1002/jbm.a.35915
30. Zhang J, Huang J, Xu S, Wang K, Yu S. Effects of Cu2+ and pH on osteoclastic bone resorption in vitro. Prog Nat Sci. 2013 Apr;13(4):266–70. https://doi.org/10.1080/10020070312331343510
31. Bosetti M, Cannas M. The effect of bioactive glasses on bone marrow stromal cells differentiation. Biomaterials. 2005 Jun;26(18):3873–9. https://doi.org/10.1016/j.biomaterials.2004.09.059
32. Hoppe A, Güldal NS, Boccaccini AR. A review of the biological response to ionic dissolution products from bioactive glasses and glass-ceramics. Biomaterials. 2011 Apr;32(11):2757–74. https://doi.org/10.1016/j.biomaterials.2011.01.004
33. Detsch R, Hagmeyer D, Neumann M, Schaefer S, Vortkamp A, Wuelling M, et al. The resorption of nanocrystalline calcium phosphates by osteoclast-like cells. Acta Biomater. 2010 Aug;6(8):3223–33. https://doi.org/10.1016/j.actbio.2010.03.003
34. Granito RN, Rennó AC, Ravagnani C, Bossini PS, Mochiuti D, Jorgetti V, et al. In vivo biological performance of a novel highly bioactive glass-ceramic (Biosilicate®): a biomechanical and histomorphometric study in rat tibial defects. J Biomed Mater Res B Appl Biomater. 2011 Apr;97(1):139–47. https://doi.org/10.1002/jbm.b.31795
35. Schroeder A, Mueller O, Stocker S, Salowsky R, Leiber M, Gassmann M, et al. The RIN: an RNA integrity number for assigning integrity values to RNA measurements. BMC Mol Biol. 2006 Jan;7(1):3. https://doi.org/10.1186/1471-2199-7-3
36. Pedersen KB, Williams A, Watt J, Ronis MJ. Improved method for isolating high-quality RNA from mouse bone with RNAlater at room temperature. Bone Rep. 2019 May;11:100211. https://doi.org/10.1016/j.bonr.2019.100211
37. Vogel C, Marcotte EM. Insights into the regulation of protein abundance from proteomic and transcriptomic analyses. Nat Rev Genet. 2012 Mar;13(4):227–32. https://doi.org/10.1038/nrg3185
38. Veronesi F, Tschon M, Fini M. Gene Expression in Osteolysis: Review on the Identification of Altered Molecular Pathways in Preclinical and Clinical Studies. Int J Mol Sci. 2017 Feb;18(3):499. https://doi.org/10.3390/ijms18030499
39. Li Z, Kong K, Qi W. Osteoclast and its roles in calcium metabolism and bone development and remodeling. Biochem Biophys Res Commun. 2006 May;343(2):345–50. https://doi.org/10.1016/j.bbrc.2006.02.147
40. Qing Hong Z, Meng Tao L, Yi Z, Wei L, Ju Xiang S, Li L. The effect of rotative stress on CAII, FAS, FASL, OSCAR, and TRAP gene expression in osteoclasts. J Cell Biochem. 2013 Feb;114(2):388–97. https://doi.org/10.1002/jcb.24372